Hydrol. Earth Syst. Sci. Discuss., 8, 8291–8314, 2011
www.hydrol-earth-syst-sci-discuss.net/8/8291/2011/
doi:10.5194/hessd-8-8291-2011

Hydrology and Earth System Sciences Discussions

Spatial and temporal variability of rainfall erosivity factor for Switzerland

K. Meusburger[1], A. Steel[2], P. Panagos[2], L. Montanarella[2], and C. Alewell[1]

[1]Institute for Environmental Geosciences, University of Basel, Bernoullistrasse 30, 4056 Basel, Switzerland
[2]Joint Research Centre of the European Commission, Institute for Environment and Sustainability, E. Fermi 2749, 21027, Ispra (VA), Italy

Received: 17 August 2011 – Accepted: 26 August 2011 – Published: 6 September 2011

Correspondence to: K. Meusburger (katrin.meusburger@unibas.ch)

Published by Copernicus Publications on behalf of the European Geosciences Union.

Abstract

Rainfall erosivity, considering rainfall amount and intensity, is an important parameter for soil erosion risk assessment under future land use and climate change. Despite its importance, rainfall erosivity is usually implemented in models with a low spatial and temporal resolution. The purpose of this study is to assess the temporal- and spatial distribution of rainfall erosivity (*R*-factor) in Switzerland. Time series of 22 yr for rainfall (10 min resolution) and temperature (1 h resolution) data were analysed for 71 automatic gauging stations distributed throughout Switzerland. Multiple regression was used to interpolate the erosivity values of single stations and to generate a map for Switzerland. Latitude, longitude, average annual precipitation, biogeographic units (Jura, Midland, etc.), aspect and elevation were used as covariates, of which average annual precipitation, elevation and the biographic unit (Western Alps) were significant predictors. The mean value of long-term rainfall erosivity is 1323 $\mathrm{MJ\,mm\,ha^{-1}\,h^{-1}\,yr^{-1}}$ with a range of lowest values of 124 $\mathrm{MJ\,mm\,ha^{-1}\,h^{-1}\,yr^{-1}}$ at an elevated station in Grisons to highest values of 5611 $\mathrm{MJ\,mm\,ha^{-1}\,h^{-1}\,yr^{-1}}$ in Ticino. All stations have highest erosivity values from July to August and lowest values in the winter month. Swiss-wide the month May to October show significantly increasing trends of erosivity ($p < 0.005$). Only in February a significantly decreasing trend of rainfall erosivity is found ($p < 0.01$). The increasing trends of erosivity in May, September and October when vegetation cover is susceptible are likely to enhance soil erosion risk for certain agricultural crops and alpine grasslands in Switzerland.

1 Introduction

Soil erosion by water in Switzerland is a major environmental threat because Switzerland is one of the countries where strongest effects of climate change are expected (Beniston, 2006; IPCC, 2007). In addition, profound land use changes occur predominantly in the susceptible mountainous areas (Meusburger and Alewell, 2008; Tasser and Tappeiner, 2002; Mottet et al., 2006). Rainfall is one of the main drivers of soil erosion by water. Climate change may lead to changes in rainfall characteristics and is thus a major concern to soil conservation. The relation between rainfall and sediment yield is given by the rainfall erosivity, which quantifies the kinetic energy of raindrop impact and rate of associated surface runoff. As field measurements of the kinetic energy of rainfall are scarce both in space and time, numerous works have assessed the relationship between conventional rainfall characteristics and soil detachment e.g. Hudson (1971) for Southern Africa, Lal (1976) for Nigeria and Arnoldus (1977) for Morocco. The most prominent and widely-used for temperate zones is probably the (R)USLE R-factor, which is the sum of all erosive events during a one year period (Brown and Foster, 1987; Renard et al., 1997; Wischmeier and Smith, 1978).

Few torrential rainfall events are often responsible for large sediment yields, these events cannot be identified from rainfall data with low temporal resolution. In the context of varying soil erosion susceptibility caused by seasonal changes in the protective vegetation cover (Panagos et al., 2011), the temporal distribution throughout the year and the timing of the most severe events is an important characteristic of rainfall erosivity. In many studies the rainfall erosivity calculation is limited to either time analysis of single stations (Mikos et al., 2006; Verstraeten et al., 2006) or for larger spatial scales to regional approximation equations (Diodato and Bellocchi, 2007; De Santos Loureiro and De Azevedo Coutinho, 2001). The original method to calculate the erosivity values for a storm event requires pluviographic records (Wischmeier, 1978). Due to limited availability of long precipitation time-series with a high temporal resolution, several alternative strategies have been deployed based on the rainfall volume (instead of intensity) for R-factor estimation. However, authors of those erosivity equations suggest using them with caution especially for the alpine region (Mikos et al., 2006). Only few studies exist that determine R-factor directly from high temporal resolution data in mountain areas of Europe (Angulo-Martinez et al., 2009; Mikos et al., 2006; Rogler and Schwertmann, 1981; Loureiro and Coutinho, 2001). For Switzerland the rainfall erosivity map is so far based on a combined approximation equation proposed by Friedli

HESSD
8, 8291–8314, 2011
Spatial and temporal variability of rainfall erosivity factor for Switzerland
K. Meusburger et al.

et al. (2006), where long-term R-factor is approximated by average annual precipitation (mm) after Rogler and Schwertmann (1981) and proportion of snowfall is approximated by elevation (m a.s.l.) after Schüpp (1975). Because rainfall erosivity is not distributed uniformly through the year, for the evaluation of soil erosion hazard continuous maps and temporal patterns of rainfall erosivity are needed. Interpolation of rainfall erosivity is challenging because of the high temporal and spatial variability of the R-factor long time series and good covariates are needed.

This study aims to evaluate the temporal as well as the spatial distribution of rainfall erosivity and to produce a map of average annual rainfall erosivity for Switzerland. We propose an automated algorithm for estimation of rainfall erosivity R-factor from high resolution precipitation- and temperature data. We further propose an adaptation of the code using temperature data to account for snowfall in elevated areas of Switzerland.

2 Materials and methods

The precipitation regime of Switzerland is characterised by a distinct seasonality with lowest precipitation in winter and highest in summer. The rainfall distribution in winter is characterised by westerly winds causing high precipitation in the north-western part and low precipitation in central and eastern parts of Switzerland. The relief of the Alps has a strong influence on precipitation and temperature. Convection events promoted by the mountainous relief are an important driver of total rainfall in summer. The south side of the Alps is characterised by high rainfall exceeding the national average for all seasons except for the relatively dry winters. Rainfall data was available for 71 automatic and heated stations in Switzerland (Fig. 1). Each station provides precipitation data at a time resolution of 10 min and temperature data at a time resolution of 1 h. For most of the stations ($n = 56$) time series of 22 yr were available. The remaining stations had a recording length of at least 5.4 yr. The data was subjected to a quality control by MeteoSchweiz (Begert et al., 2005). The stations are well distributed throughout Switzerland (Fig. 1) and represent different geographical zones and climate regions.

HESSD
8, 8291–8314, 2011

2.1 Computation of rainfall erosivity

The RUSLE R-factor was employed to create a database of erosive events. RUSLE R-factor is the product of kinetic energy of a rainfall event and its maximum 30-min intensity (Brown and Foster, 1987):

$$R = \frac{1}{n}\sum_{j=1}^{n}\sum_{k=1}^{m_j}(\mathrm{EI}_{30})_k \tag{1}$$

where R-factor is average annual rainfall erosivity (MJ mm ha^{-1} h^{-1} y^{-1}), n is the number of years of records, m_j is the number of erosive events of a given year j, and EI_{30} is the rainfall erosivity index of a single event k. The event erosivity EI_{30} (MJ mm ha^{-1} h^{-1}) is defined as:

$$\mathrm{EI} = \mathrm{EI}_{30} = \left(\sum_{r=1}^{0} e_r v_r\right) I_{30} \tag{2}$$

where e_r is the unit rainfall energy (MJ ha^{-1} mm^{-1}) and the v_r the rainfall volume (mm) during a time period r. I_{30} is the maximum rainfall intensity during a period of 30 min in the event (mm h^{-1}). The unit rainfall energy is calculated for each time interval as follows:

$$e_r = 0.29[1 - 0.72\exp(-0.05 i_r)] \tag{3}$$

where i_r is the rainfall intensity during the time interval (mm h^{-1}). In addition to the R-factor we calculated monthly sums of EI_{30}.

The criteria for the identification of an erosive event are given by Renard et al. (1997): (i) the cumulative rainfall of an event should be greater than 12.7 mm, or (ii) the event has at least one peak that is greater than 6.35 mm in 15 min and (iii) a rainfall-period of less than 1.27 mm in 6 h is used to divide a longer storm period into two storms.

HESSD
8, 8291–8314, 2011

In our code we modified the second criteria of Renard et al. (1997). A threshold of 8.47 mm/20 min instead of 6.35 mm/15 min was used in order to best fit to the time resolution of the precipitation data (10 min). Of course the likelihood to observe an 8.47 mm/20min event is slightly smaller than a 6.35 mm/15 min event. However, the additional number of erosive events due to this intensity criteria is marginal (only two stations had additional events due to the intensity criteria). Several stations are elevated and a large proportion of the annual precipitation occurs as snowfall that the heated stations measure erroneously as rainfall. Therefore a temperature threshold, below which precipitation records are not considered when searching for rainfall events was used. Here we applied a temperature threshold of 0 °C (Leek and Olsen, 2000).

The algorithm was implemented in C programming language. The proposed algorithm can be reused for other local/regional/national applications where rainfall data and temperature data are available with the same temporal resolution.

2.2 Rainfall erosivity mapping for Switzerland

The dataset consists of 71 stations for an area of 41 285 km^2. Multiple regression was used to interpolate the at-site estimated R-factor to a map. The purpose of the regression was to identify relations between the target variable (here: R-factor) and other variables with a better spatial resolution (covariates). The resulting residual map may be interpolated by kriging and added to the regression map in order to improve the spatial prediction. Regression-based methods have proved to be suitable for large regions with complex atmospheric conditions and with sparse sample network (Weisse and Bois, 2002; Daly et al., 2002). The elevation, aspect (digital elevation model of Swisstopo, 25 m spatial resolution), latitude, longitude, average (1971–1990) annual precipitation map with a resolution of 1.25 min (Schwarb, 2000), and the main biogeographic units of Switzerland (Gonseth et al., 2001) were used as covariates. The biogeographic unit map is the only categorical variable (6 categories: namely Jura, Midland, north side of the Alps, south side of the Alps, Western and Eastern Central Alps) and was transformed to indicator maps.

HESSD
8, 8291–8314, 2011

For the regression analysis the variance inflation factor (vif) was used to assess multicollinearity between the covariates. Further the covariates were normalised (standard score) and the *R*-factor was log-transformed to achieve a normal distribution. A static semivariogram model was used to parameterise the spatial autocorrelation between the residuals coming from the regression analysis. Non-constant error variance test was used to assess homoscedasticity of the residuals. Prior to the regression procedure a stratified split into calibration (53 stations) and validations datasets (18 stations) was done. The validation data was selected in such a way to both represent the entire study area and to decluster the dataset (Fig. 1).

The multiple regression was done with *R* statistical analysis package (R Development Core Team, v. 2.13), the geostatistical analyses were done in Esri ArcGIS 10.

2.3 Trend analysis

A minimum time period of 20–25 yr is recommended for the calculation of a long-term *R*-factor (Wischmeier, 1987; Renard, 1997). However, these time series might not be long enough for trend analysis due to the high temporal variability of rainfall erosivity. A Seasonal Mann-Kendall test (Hirsch et al., 1982) was used to test for significant monotonic trends of rainfall erosivity at stations with data for 22 yr. A Mann-Kendall trend test was used to identify trends for individual month of all stations (Mann, 1945). The seasonal variability of rainfall erosivity is illustrated by monthly regime coefficients, which are the monthly erosivity values divided by the average yearly erosivity.

3 Results and discussion

3.1 Erosivity map of Switzerland

The long-term *R*-factor is significantly related to average annual precipitation ($p < 0.001$) and to elevation ($p < 0.01$). The indicator map of the Western Central Alps

(Canton Valais) was another significant predictor ($p < 0.01$) Covariates as latitude, longitude, aspect and the other biogeographic units were no significant predictors for rainfall erosivity. The following regression equation was used to interpolate the erosivity values of the single stations:

$$\log R = 0.4989 nP - 0.2755 n\text{dem} - 0.6873\text{west} + 7.624 \quad (4)$$

where nP is the normalized average annual precipitation, $n$dem the normalized elevation and west the biogeographic unit indicator map of the Western Central Alps. The multiple regression could explain 79.6 % of the observed spatial variability of the calibration dataset and 89.4 % of the validation dataset (Fig. 2 left). The residuals of the model are normally distributed and a non-constant error variance test confirmed homoscedasticity of the residuals. The vif indicated a collinearity between average annual precipitation and elevation (vif < 3.3). However, regression models based on either annual precipitation or elevation yielded lower R^2 values and heteroscedasticity of the residuals.

The residuals derived from the regression analysis were interpolated by kriging using a stable semivariogram model. Positive residuals indicate an underestimation of the R-factor particularly in the Bernese Alps and negative residuals an overestimation particularly in the Central Alps (Fig. 3). The estimates of the regression model and the krigged residuals were added to produce a regression-kriging prediction. The predictions of the regression-kriging for the validation dataset performed worse than for the regression model alone (Fig. 2 right). Further, the residuals resulting from the regression-kriging prediction were not normal distributed.

Several techniques for mapping the rainfall erosivity have been compared by Angulo-Martinez et al. (2009) for a study site in Spain (Ebro basin 85 000 km^2) using precipitation data of 112 stations. Concerning the validation statistics local interpolation methods like Inverse Distance Weighting (IDW) performed best for the Ebro basin. Compared to spline and krigging interpolation, IDW performed also best for a study area in Japan (Santosa et al., 2010). One explanation might be the lack of significant relations

HESSD
8, 8291–8314, 2011

Spatial and temporal variability of rainfall erosivity factor for Switzerland

K. Meusburger et al.

between rainfall erosivity and spatial covariates. For the Swiss dataset the predictive power of the covariates is good, thus, the regression-based interpolation seemed to be the best choice for the final Swiss rainfall erosivity map (Fig. 4).

The mean erosivity of Switzerland is 1323 MJ mm ha^{-1} h^{-1} y^{-1} with a maximum of 5611 MJ mm ha^{-1} h^{-1} y^{-1} at the station Locarno Monti in Ticino (south side of the Alps) and a minimum of 124 MJ mm ha^{-1} h^{-1} y^{-1} at the station Corvatsch in Grisons (Eastern Central Alps). In general, Ticino is the region with the highest rainfall erosivity followed by elevated stations North of the Alps (e.g. Säntis, Adelboden; Fig. 4). Medium level erosivities are observed in the north-western part of Switzerland. The regions with the lowest rainfall erosivities are the Valais and Grisons (Fig. 4). An overview of the R-factor for each station is given in Table 1.

The average R-factor values found for Switzerland are similar to the ones published by Mikos et al. (2006) for Slovenia, which range from 1580 to 2700 MJ mm ha^{-1} h^{-1} y^{-1} for different years of one station. However, the Ticino values are twice as high as the maximum value observed for the Slovenian station, which can be explained by higher annual precipitation means (> 1700 mm compared to 1370 mm in Slovenia) and by the strong influence of orographic rainfall in Ticino. Surprisingly small erosivity values occur in the western and eastern parts of Switzerland, which is mainly due to a very low annual precipitation in combination with a high proportion of snowfall (identified by the temperature controlled snowfall threshold).

The relationship between the obtained erosivity map and the former map after the approximation equation of Rogler and Schwertmann (1981), which was adapted to Switzerland by Friedli et al. (2006) and Prasuhn et al. (2007) can be described by a linear equation (R^2adj. = 0.66; Fig. 5). Even though the spatial pattern according to the latter equation corresponds well, the rainfall erosivity is generally underestimated: average R-factor for all Swiss stations is 775 MJ mm ha^{-1} h^{-1} y^{-1}, which is 41 % less than the R-factor determined using the original equation with the high temporal resolution data. The highest underestimation occurs for stations with high rainfall erosivity particularly in the Ticino (e.g. Locarno/Monti, Magadino/Cadenazzo, Stabio etc.). A slight

HESSD
8, 8291–8314, 2011

overestimation is observed for stations in the West and Central Alps (e.g. Visp, Grimsel Hospitz, Altdorf and Sion). The equation of Rogler and Schwertmann (1981) was developed in the Bavarian Alps (Germany) and seems to be limitedly transferable to the Ticino and Valais region due to the strong influence of orographic effects.

3.2 Temporal variability of rainfall erosivity

Annual R-factor for the period 1989 to 2010 shows distinct inter-annual variability (Fig. 6). The coefficient of variation is large (45 % for Bern, 36 % for Cimetta), especially for the stations with lower R-factor (59 % for Samedan and 55 % for Basel, respectively). This high variability is most likely the reason why seasonal Mann Kendall trend test of single stations (with data available for 22 yr) could not identify significant trends in rainfall erosivity. Even no significant trend was found for a much longer time series of 105 yr in Belgium (Verstraeten et al., 2006).

To extract the intra-annual variability of rainfall erosivity, rainfall erosivity regimes were calculated. The regimes were grouped into biogeographic regions (Fig. 7). Independent of the different biographic regions the rainfall erosivity is characterized by a strong seasonality with highest regime coefficients in the summer month (May to September) and lowest in the winter month (December to March). For elevated stations the rainfall erosivity in summer month is 3 to 5 times higher than the average yearly rainfall erosivity, due to the long snowfall season e.g. station Corvatsch (3350 m a.s.l.). For most stations rainfall erosivity peaks in July or (particularly in the Jura and the Northern Alps) in August. Mann-Kendall trend test for single months over the 22 investigated years identified a significant increasing trend of rainfall erosivity for May to October and a significant decreasing trend for February (Table 2).

The erosivity regimes clearly highlight the importance of monthly rainfall erosivity maps for soil erosion risk assessment, because even a decline in precipitation volume may result in higher rainfall erosivity for some month (Marker et al., 2008). Furthermore, changes in rainfall erosivity cannot be directly linked to soil erosion risk because of the seasonal variability of vegetation cover. According to our results, three out of the six

HESSD
8, 8291–8314, 2011

month with significant increasing trends can also be expected to have relatively sparse or instable vegetation cover. Most cultivated areas (e.g. winter crop, corn, vegetable fields) as well as Alpine grasslands will have low vegetation cover in May and will be harvested/grazed in September/October and will thus be susceptible to erosion during snow melt and/or heavy rain events. Consequently the increased rainfall erosivity in May, September and October will most likely result in an increased soil erosion risk for Switzerland.

4 Conclusion and outlook

The R-factor was successfully mapped using a multiple regression (R^2 adj. = 0.89 and R^2 adj. = 0.79 for the validation and calibration dataset, respectively). The implementation of associated temperature data could improve the rainfall erosivity estimates for mountain areas. However, in mountain areas there is still a great demand for research on erosivity caused by snowmelt, snowgliding and avalanches, which is not yet accounted for a further challenge will be the Swiss-wide mapping of monthly rainfall erosivities.

The analysis of both the spatial and temporal pattern of rainfall erosivity yielded crucial new information for soil erosion assessment in Switzerland: (i) rainfall erosivity is on average 71 % higher as expected from the former applied approximation equation proposed by Friedli et al. (2006) and (ii) the rainfall erosivity significantly increased in the period of May to October (1989–2010). The latter result of this study indicate that climatic change may have a significant impact on soil erosion. The seasonal pattern of increase particularly in May, September and October might lead to a higher soil erosion risk for certain agricultural crops (e.g. corn, winter crops, vegetable fields) and for Alpine grassland. Therefore, changes in seasonality should be included in soil erosion risk assessment and future land use management.

HESSD
8, 8291–8314, 2011

Acknowledgement. This study was funded by the Swiss Federal Office for the Environment in the framework f the Colaboration Agreement No. 31576. Special thanks go to F. Carré for her introduction to regression-kriging.

References

Angulo-Martínez, M., López-Vicente, M., Vicente-Serrano, S. M., and Beguería, S.: Mapping rainfall erosivity at a regional scale: a comparison of interpolation methods in the Ebro Basin (NE Spain), Hydrol. Earth Syst. Sci., 13, 1907–1920, doi:10.5194/hess-13-1907-2009, 2009.

Arnoldus, H. M. J.: Methodology used to determine the maximum potential average annual soil loss due to sheet and rill erosion in Morocco, FAO Soils Bull., 34, 39–51, 1977.

Begert, M., Schlegel, T., and Kirchhofer, W.: Homogeneous Temperature and Precipitation Series of Switzerland from 1864 to 2000, Int. J. Climatol., 25, 65–800, 2005.

Beniston, M.: Mountain weather and climate: a general overview and a focus on climatic change in the Alps, Hydrobiologia, 562, 3–16, 2006.

Brown, L. C. and Foster, G. R.: Storm erosivity using idealized intensity distributions, Trans. ASAE, 30, 379–386, 1987.

Daly, C., Gibson, W. P., Taylor, G. H., Johnson, G. L., and Pasteris, P.: A knowledge-based approach to the statistical mapping of climate, Clim. Res., 22, 99–113, doi:10.3354/cr022099, 2002.

De Santos Loureiro, N. and De Azevedo Coutinho, M.: A new procedure to estimate the RUSLE EI30 index, based on monthly rainfall data and applied to the Algarve region, Portugal, J. Hydrol., 250, 12–18, 2001.

Diodato, N. and Bellocchi, G.: Estimating monthly (R)USLE climate input in a Mediterranean region using limited data, J. Hydrol., 345, 224–236, doi:10.1016/j.jhydrol.2007.08.008, 2007.

Friedli, S.: Digitale Bodenerosionsgefährdungskarte der Schweiz im Hektarraster – unter besonderer Berücksichtigung des Ackerlandes, Diplomarbeit Geogr. Inst. Univ. Bern und Agroscope FAL Reckenholz, 110 pp., 2006.

Gonseth, Y., Wohlgemuth, T., Sansonnens, B., and Buttler, A.: Die biogeographischen Regionen der Schweiz. Erläuterungen und Einteilungsstandard, Bundesamt für Umwelt, Wald und Landschaft Bern, 48, 2001.

Hirsch, R. M., Slack, J. R., and Smith, R. A.: Techniques of trend analysis for monthly water quality data, Water Resour. Res., 18, 107–121, 1982.
Hudson, N.: Cornell University Press, Soil Conservation, Ithaca, 1971.
IPCC: Climate Change 2007: The Physical Science Basis. Summary for Policymakers, 661, 10th Session of Working Group I of the IPCC, Paris, 2007.
Lal, R.: Soil erosion on alfisols in Western Nigeria. III – Effects of rainfall characteristics, Geoderma, 16, 389–401, 1976.
Leek, R. and Olsen, P.: Modelling climatic erosivity as a factor for soil erosion in Denmark: changes and temporal trends, Soil Use Manage., 16, 61–65, 2000.
Loureiro, N. D. and Coutinho, M. D.: A new procedure to estimate the RUSLE EI30 index, based on monthly rainfall data and applied to the Algarve region, Portugal, J. Hydrol., 250, 12–18, 2001.
Mann, H. B.: Nonparametric tests against trend, Econometrica, 13, 245–259, 1945.
Marker, M., Angeli, L., Bottai, L., Costantini, R., Ferrari, R., Innocenti, L., and Siciliano, G.: Assessment of land degradation susceptibility by scenario analysis: A case study in Southern Tuscany, Italy, Geomorphology, 93, 120–129, doi:10.1016/j.geomorph.2006.12.020, 2008.
Meusburger, K. and Alewell, C.: Impacts of anthropogenic and environmental factors on the occurrence of shallow landslides in an alpine catchment (Urseren Valley, Switzerland), Nat. Hazard Earth Sys., 8, 509–520, 2008.
Mikos, M., Jost, D., and Petkovsek, G.: Rainfall and runoff erosivity in the alpine climate of North Slovenia: a comparison of different estimation methods, Hydrol. Sci. J., 51, 115–126, 2006.
Mottet, A., Ladet, S., Coque, N., and Gibon, A.: Agricultural land-use change and its drivers in mountain landscapes: a case study in the Pyrenees, Agr. Ecosyst. Environ., 114, 296–310, 2006.
Panagos, P., Karydas, C. G., Gitas, I. Z., and Montanarella, L.: Monthly soil erosion monitoring based on remotely sensed biophysical parameters: a case study in Strymonas river basin towards a functional pan-European service, Int J. Digital Earth, doi:10.1080/17538947.2011.587897, in press, 2011.
Prasuhn, V., Liniger, H., Hurni, H., and Friedli, S.: Map of soil erosion risk in Switzerland, Agrarforschung, 14, 120–127, 2007.
Renard, K. G., Foster, G. R., and Weesies, G. A.: Predicting soil erosion by water; a guide to conservation planning with the revised universal soil loss equation (RUSLE), Agriculture

HESSD
8, 8291–8314, 2011

Handbook No. 703, USDA-ARS, 404 pp., 1997.
Rogler, H. and Schwertmann, U.: Rainfall erosivity and isoerodent map of Bavaria, Z. Kulturtechnik Flurbereinigung, 22, 99–112, 1981.
Santosa, P. B., Mitani, Y., and Ikemi, H.: Estimation of RUSLE EI 30 based on 10 min interval rainfall data and GIS-based development of rainfall erosivity maps for Hitotsuse basin in Kyushu Japan, 18th International Conference on Geoinformatics, 2010, INSPEC:11532406, 2010.
Schüpp, M.: Objective weather forecasts using statistical aids in Alps, Riv. Ital. Geofis. Sci., 1, 32–36, 1975.
Schwarb, M.: The alpine precipitation climate. The alpine precipitation evaluation of a high-resolution analysis scheme using comprehensive rain-gauge data, Doctoral and Habilitation Theses. Diss. ETHNo, 13911, Swiss Federal Institue of Technology, Zürich 2000.
Tasser, E. and Tappeiner, U.: Impact of land use changes on mountain vegetation, 5, 173–184, 2002.
Verstraeten, G., Poesen, J., Demaree, G., and Salles, C.: Long-term (105 years) variability in rain erosivity as derived from 10-min rainfall depth data for Ukkel (Brussels, Belgium): implications for assessing soil erosion rates, J. Geophys. Res.-Atmos., 111(11), D22109, doi:10.1029/2006jd007169, 2006.
Weisse, A. K. and Bois, P.: A comparison of methods for mapping statistical characteristics of heavy rainfall in the French Alps: the use of daily information, Hydrol. Sci. J., 47, 739–752, doi:10.1080/02626660209492977, 2002.
Wischmeier, W. H. and Smith, D. D.: Predicting Rainfall Erosion Losses – A Guide to Conservation Planning. Agric. Handbook No. 537, Washington DC, 58, 1978.

HESSD
8, 8291–8314, 2011

Spatial and temporal variability of rainfall erosivity factor for Switzerland

K. Meusburger et al.

Table 1. Average annual *R*-factor ($MJ\,mm\,ha^{-1}\,h^{-1}\,y^{-1}$) and descriptive statistics of the event's rainfall erosivity ($MJ\,mm\,ha^{-1}\,h^{-1}$) for single stations.

Station	Acronym	*R*-factor	Length of time series (year)	Missing data (%)	Mean EI_{30}	Stdev. EI_{30}	Max. EI_{30}
Adelboden	ABO	2143.0	22.0	0.3	39.0	75.6	710.5
Aigle	AIG	758.4	22.0	0.2	32.8	67.1	1162.8
Altdorf	ALT	921.2	22.0	0.1	35.7	98.2	1500.7
Basel/Binningen	BAS	853.3	22.0	0.9	57.0	119.1	1101.9
Bern/Zollikofen	BER	1052.0	22.0	0.8	47.6	79.7	698.3
Beznau	BEZ	648.3	22.0	0.4	31.2	69.4	966.8
Buffalora	BUF	370.4	11.8	0.6	30.0	41.4	339.6
Buchs/Aarau	BUS	937.4	22.0	0.3	45.0	76.4	675.8
La Chaux-de-Fonds	CDF	1445.2	22.0	0.4	46.4	143.2	3072.8
Nyon/Changins	CGI	863.4	22.0	0.9	38.1	90.0	1114.3
Chasseral	CHA	865.9	22.0	0.1	49.5	81.3	697.4
Chur	CHU	578.0	22.0	0.1	34.6	72.6	1074.8
Cham	CHZ	746.4	17.4	0.6	43.9	69.2	671.1
Cimetta	CIM	3810.6	22.0	1.3	150.5	291.7	2517.2
Acquarossa/Comprovasco	COM	1727.1	22.0	0.9	73.5	164.9	2763.6
Piz Corvatsch	COV	123.9	22.0	1.2	30.0	25.1	132.5
Davos	DAV	644.8	22.0	0.1	34.8	48.4	621.0
Disentis/Sedrun	DIS	714.2	22.0	0.4	40.8	62.4	518.0
La Dôle	DOL	1652.0	22.0	0.3	51.8	76.9	694.9
Engelberg	ENG	1162.2	22.0	0.3	35.6	48.4	461.0
Evolène/Villa	EVO	319.3	22.0	1.0	31.6	99.0	1392.1
Fahy	FAH	918.7	22.0	0.1	42.2	78.9	742.4
Bullet/La Fraz	FRE	1314.4	22.0	1.3	48.2	124.4	1962.3
Monte Generoso	GEN	3282.5	15.0	5.0	153.9	305.5	2761.1
Glarus	GLA	1272.7	22.0	0.3	36.2	66.3	1237.4
Goesgen	GOE	822.3	22.0	0.3	39.0	74.0	658.7
Grimsel Hospiz	GRH	495.3	21.5	0.9	30.1	59.8	741.6
Col du Grand St-Bernard	GSB	965.9	22.0	0.3	59.1	117.5	1474.1
Guetsch ob Andermatt	GUE	521.4	22.0	0.4	45.8	67.8	442.8
Guettingen	GUT	864.2	22.0	0.8	45.5	87.2	825.9
Genève-Cointrin	GVE	812.7	22.0	0.4	37.7	60.5	691.3
Hinterrhein	HIR	1956.8	20.1	0.3	77.8	122.8	1035.8
Hoernli	HOE	1035.2	5.4	0.6	37.6	63.9	547.2
Interlaken	INT	1034.6	22.0	0.4	38.3	68.2	866.7
Zuerich/Kloten	KLO	1291.0	6.8	0.0	53.8	99.3	789.1

HESSD
8, 8291–8314, 2011

Table 1. Continued.

Station	Acronym	*R*-factor	Length of time series (year)	Missing data (%)	Mean EI_{30}	Stdev. EI_{30}	Max. EI_{30}
Leibstadt	LEI	619.4	22.0	0.2	29.0	50.5	504.6
Lugano	LUG	4672.7	22.0	0.1	138.2	306.3	4625.9
Luzern	LUZ	1592.6	22.0	0.4	58.6	107.6	1412.7
Magadino/Cadenazzo	MAG	5032.5	22.0	0.3	160.9	313.8	3657.1
Mathod	MAH	1021.9	18.3	1.3	82.9	250.0	2440.0
Montana	MVE	362.18	22.0	0.1	23.6	26.9	251.2
Napf	NAP	1878.4	22.0	1.1	60.2	114.6	1176.6
Neuchael	NEU	932.8	22.0	0.3	46.3	114.1	1528.4
Locarno Monti	OTL	5611.0	22.0	0.8	178.0	445.0	5603.9
Payerne	PAY	834.5	22.0	0.1	47.6	133.9	2069.3
Pilatus	PIL	1054.2	22.0	0.3	61.2	122.0	1400.5
Piotta	PIO	1694.5	22.0	0.0	70.8	115.0	884.5
Plaffeien	PLF	1571.3	21.1	0.7	57.0	98.4	997.2
PSI Wuerenlingen	PSI	677.5	18.8	0.0	30.9	56.2	771.2
Pully	PUY	1192.7	22.0	0.3	47.1	83.5	741.3
Zuerich/Affoltern	REH	1283.6	6.8	0.0	54.9	140.7	1609.4
Poschiavo/Robbia	ROB	913.0	22.0	0.1	41.2	74.9	821.0
Robièi	ROE	2721.4	19.9	1.5	93.7	159.6	1596.2
Ruenenberg	RUE	917.7	22.0	0.3	46.6	97.4	1146.5
Saetis	SAE	2362.9	22.0	0.6	99.2	309.4	5484.1
Samedan	SAM	339.9	22.0	0.1	25.7	32.6	381.7
S. Bernardino	SBE	2008.7	22.0	1.0	71.0	110.1	1029.3
Stabio	SBO	4708.1	22.0	0.3	153.2	347.6	5686.3
Scuol	SCU	489.9	22.0	0.2	36.6	97.6	1274.1
Schaffhausen	SHA	744.0	22.0	0.7	41.8	95.0	1254.3
Sion	SIO	278.5	22.0	0.4	22.5	28.3	225.8
Zuerich/Fluntern	SMA	1090.5	22.0	0.8	45.8	83.7	781.9
St. Gallen	STG	1499.4	22.0	0.3	55.0	106.2	1555.1
Aadorf/Taenikon	TAE	1374.2	22.0	0.9	49.4	100.6	1184.9
Ulrichen	ULR	642.9	22.0	0.3	32.8	46.8	388.4
Vaduz	VAD	810.0	22.0	0.1	41.9	112.1	1498.5
Visp	VIS	223.3	22.0	0.4	22.4	33.3	245.6
Waedenswil	WAE	1658.2	22.0	0.9	50.7	122.6	2589.0
Weissfluhjoch	WFJ	654.5	6.8	0.0	43.4	60.8	552.5
Wynau	WYN	1350.6	6.8	0.0	55.0	103.4	779.4
Zermatt	ZER	207.4	6.8	0.0	25.5	27.5	172.7

HESSD
8, 8291–8314, 2011

Table 2. Mann-Kendall trend test for single month for all Swiss stations. Tau is the Mann-Kendall rank correlation coefficient.

Month	tau	2-sided p-value
Jan	0.015	0.453
Feb	−0.052	0.006
Mar	0.033	0.045
Apr	0.030	0.041
May	0.047	0.000
Jun	0.032	0.003
Jul	0.040	0.000
Aug	0.038	0.001
Sep	0.055	0.000
Oct	0.040	0.001
Nov	0.018	0.211
Dec	−0.001	0.493

HESSD
8, 8291–8314, 2011

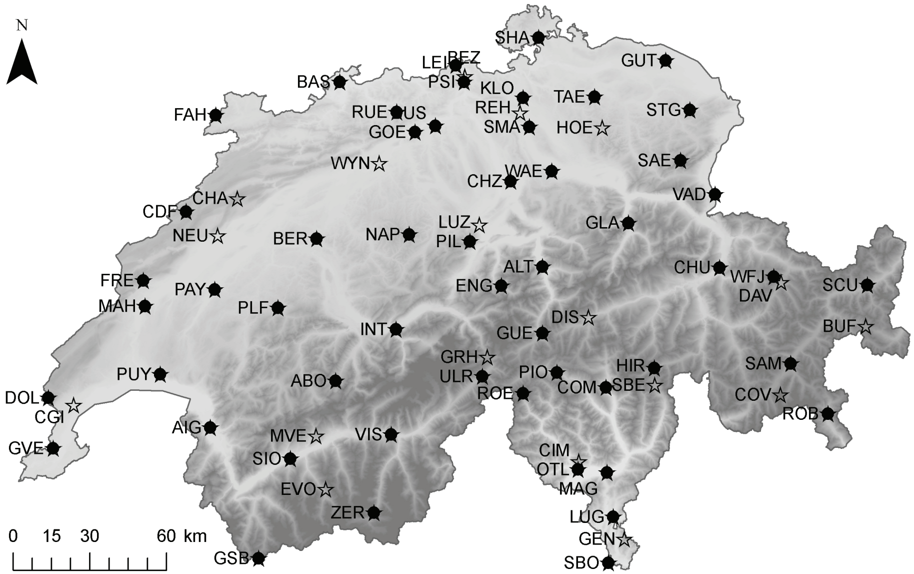

Fig. 1. Location of automatic rainfall stations in Switzerland (star dots are stations used for the validation of the rainfall erosivity map).

HESSD
8, 8291–8314, 2011

Spatial and temporal variability of rainfall erosivity factor for Switzerland

K. Meusburger et al.

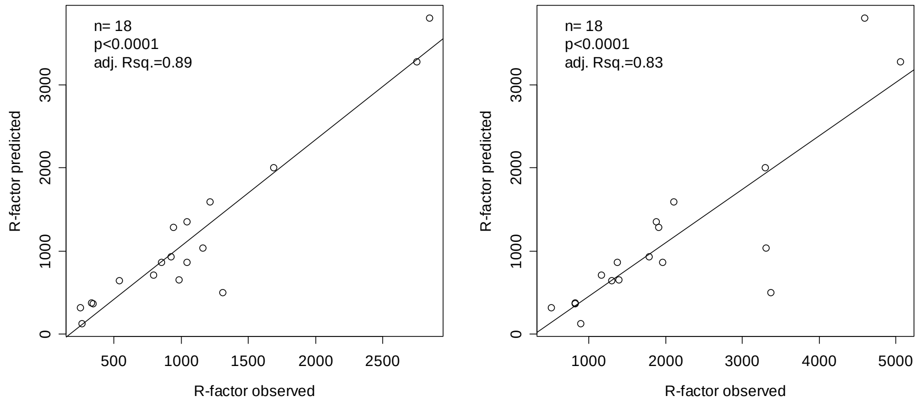

Fig. 2. Scatterplot between observed and predicted rainfall erosivity values for the validation dataset: after the regression (left) and after the regression-kriging (right).

HESSD
8, 8291–8314, 2011

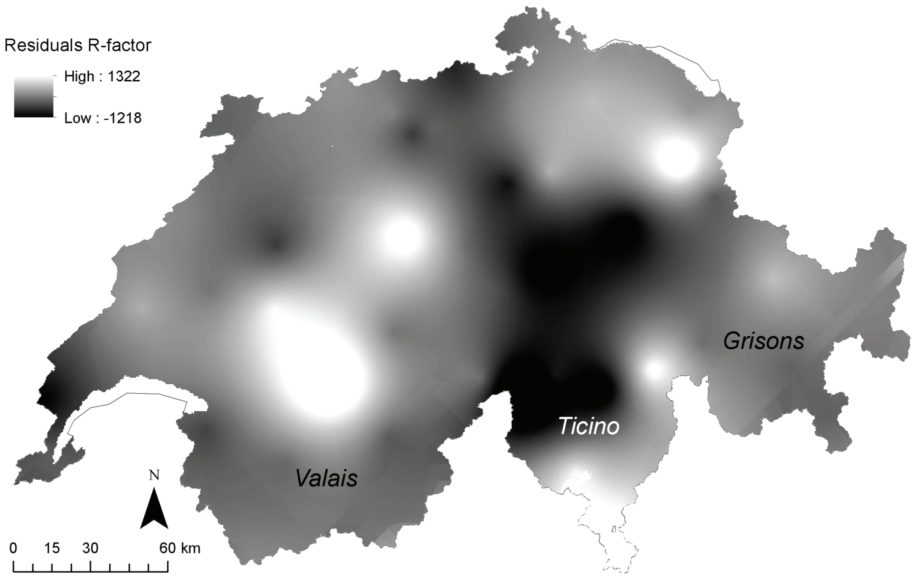

Fig. 3. Residuals of the regression interpolation of *R*-factor values.

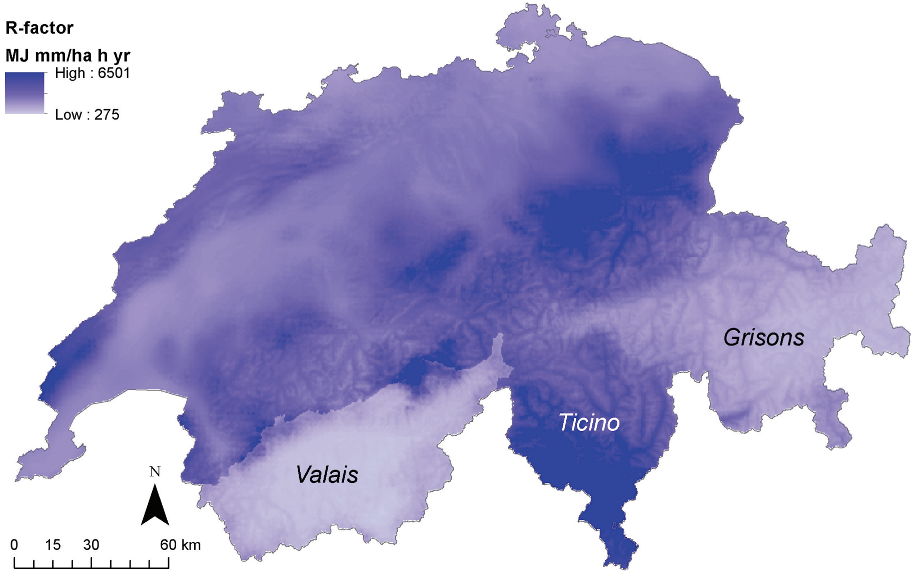

Fig. 4. Rainfall erosivity map of Switzerland resulting from regression-based interpolation of 71 stations.

HESSD
8, 8291–8314, 2011

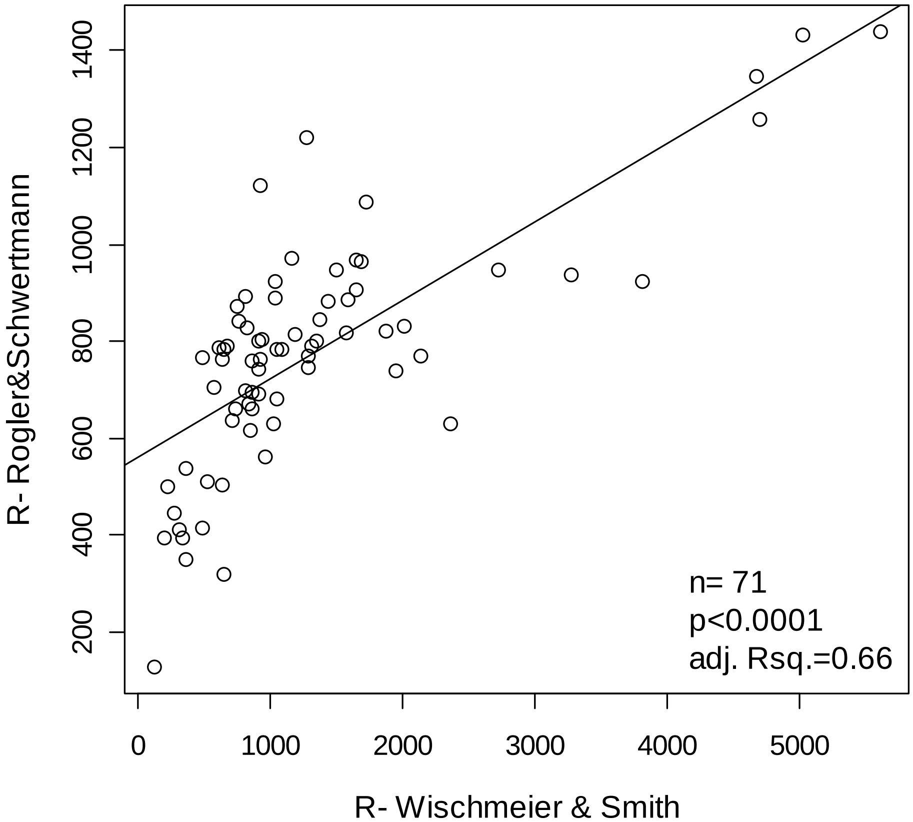

Fig. 5. Comparison or *R*-factor calculated from 10 min data versus *R*-factor based on average annual rainfall using the approximation equation of Rogler and Schwertmann (1981).

HESSD
8, 8291–8314, 2011

Spatial and temporal variability of rainfall erosivity factor for Switzerland

K. Meusburger et al.

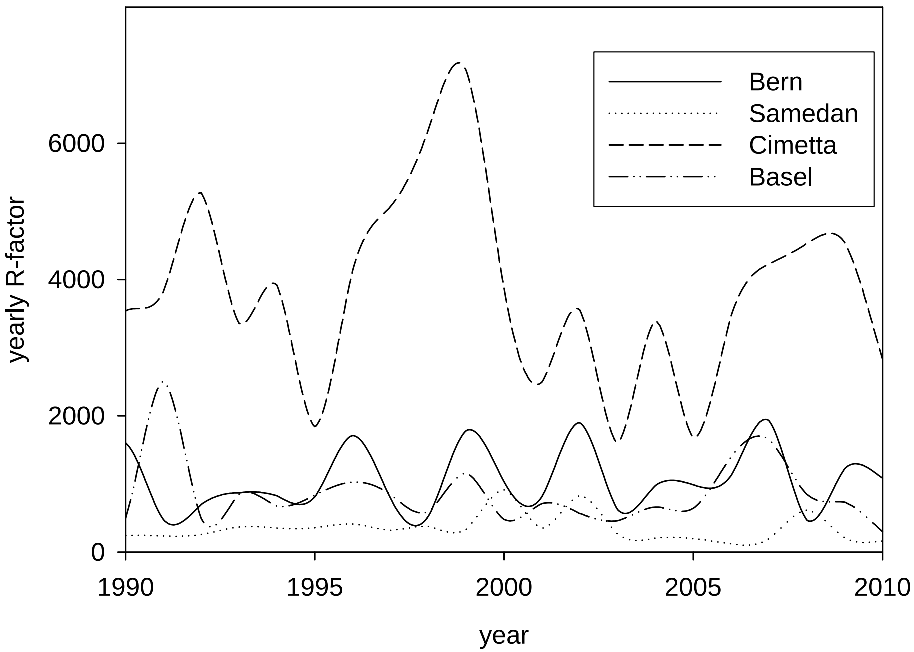

Fig. 6. Annual variability of *R*-factor for a station in Ticino (Cimetta), Grisons (Samedan) and two stations on the North side of the Alps (Bern, Basel).

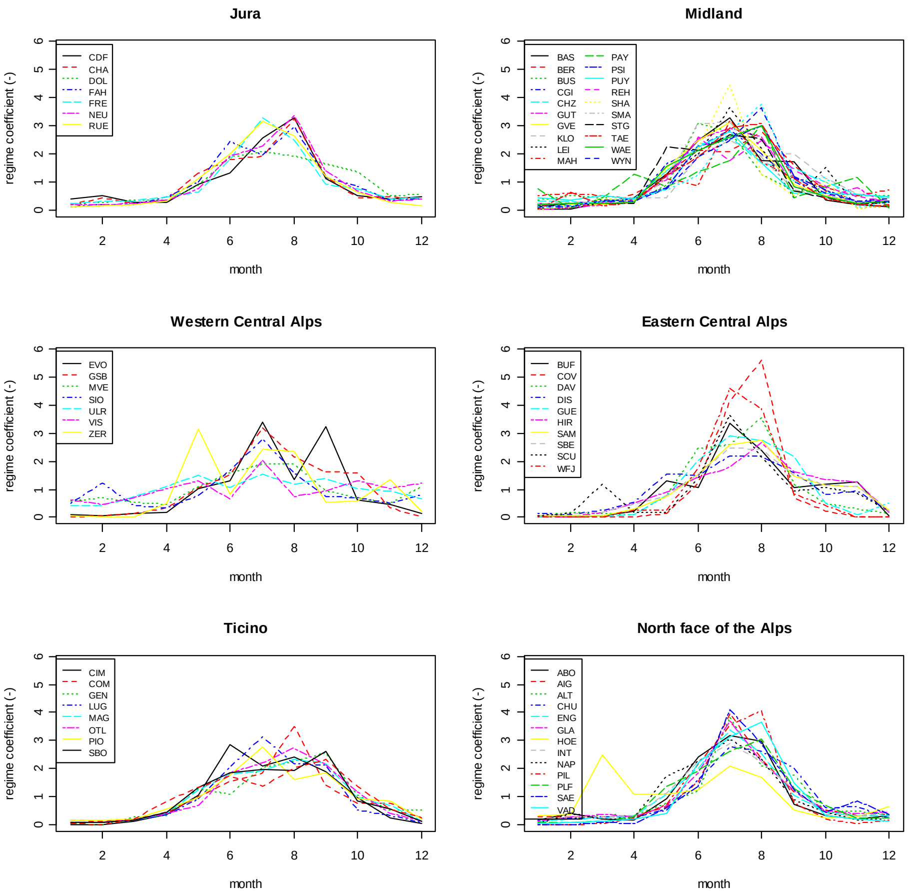

Fig. 7. Erosivity regimes grouped by biogeographic units.

HESSD

8, 8291–8314, 2011

Spatial and temporal variability of rainfall erosivity factor for Switzerland

K. Meusburger et al.

Title Page
Abstract Introduction
Conclusions References
Tables Figures
◀ ▶
Back Close
Full Screen / Esc
Printer-friendly Version
Interactive Discussion